J|A|C|S
ARTICLES
Published on Web 04/10/2004

Characterization of Fluxional Hydrogen-Bonded Complexes of Acetic Acid and Acetate by NMR: Geometries and Isotope and Solvent Effects

Peter M. Tolstoy,[†,‡] Parwin Schah-Mohammedi,[†] Sergei N. Smirnov,[‡] Nikolai S. Golubev,[‡] Gleb S. Denisov,[‡] and Hans-Heinrich Limbach*[,†]

Contribution from the Institut für Chemie, Freie Universität Berlin, Takustrasse 3, D-14195 Berlin, Germany, and the Institute of Physics, St. Petersburg State University, 198504 St. Petersburg, Russian Federation

Received October 28, 2003; E-mail: limbach@chemie.fu-berlin.de

Abstract: ^{1}H, ^{2}H, and ^{13}C NMR spectra of enriched $CH_3{}^{13}COOH$ acid without and in the presence of tetra-*n*-butylammonium acetate have been measured around 110 K using a liquefied Freon mixture CDF_3/CDF_2-Cl as a solvent, as a function of the deuterium fraction in the mobile proton sites. For comparison, spectra were also taken of the adduct $CH_3{}^{13}COOH{\cdot}SbCl_5$ **1** and of $CH_2Cl{}^{13}COOH$ under similar conditions, as well as of $CH_3{}^{13}COOH$ and $CH_3{}^{13}COO^-$ dissolved in H_2O and D_2O at low and high pH at 298 K. The low temperatures employed allowed us to detect several well-known and novel hydrogen-bonded complexes in the slow hydrogen bond exchange regime and to determine chemical shifts and coupling constants as well as H/D isotope effects on chemical shifts from the fine structure of the corresponding signals. The measurements show that self-association of both carboxylic acids in Freon solution gives rise exclusively to the formation of cyclic dimers **2** and **3** exhibiting a rapid degenerate double proton transfer. For the first time, a two-bond coupling of the type $^{2}J(CH_3COOH)$ between a hydrogen-bonded proton and the carboxylic carbon has been observed, which is slightly smaller than half of the value observed for **1**. In addition, the ^{1}H and ^{2}H chemical shifts of the HH, HD, and the DD isotopologues of **2** and **3** have been determined as well as the corresponding HH/HD/DD isotope effects on the ^{13}C chemical shifts. Similar "primary", "vicinal", and "secondary" isotope effects were observed for the novel 2:1 complex "dihydrogen triacetate" **5** between acetic acid and acetate. Another novel species is the 3:1 complex "trihydrogen tetraacetate" **6**, which was also characterized by a complex degenerate combined hydrogen bond- and proton-transfer process. For comparison, the results obtained previously for hydrogen diacetate **4** and hydrogen maleate **7** are discussed. Using an improved ^{1}H chemical shift−hydrogen bond geometry correlation, the chemical shift data are converted into hydrogen bond geometries. They indicate cooperative hydrogen bonds in the cyclic dimers; i.e., widening of a given hydrogen bond by H/D substitution also widens the other coupled hydrogen bond. By contrast, the hydrogen bonds in **5** are anticooperative. The measurements show that ionization shifts the ^{13}C signal of the carboxyl group to low field when the group is immersed in water, but to high field when it is embedded in a polar aprotic environment. This finding allows us to understand the unusual ionization shift of aspartate groups in the HIV-pepstatin complex observed by Smith, R.; Brereton, I. M.; Chai, R. Y.; Kent, S. B. H. *Nature Struct. Biol.* **1996**, *3*, 946. It is demonstrated that the Freon solvents used in this study are better environments for model studies of amino acid interactions than aqueous or protic environments. Finally, a novel correlation of the hydrogen bond geometries with the H/D isotope effects on the ^{13}C chemical shifts of carboxylic acid groups is proposed, which allows one to estimate the hydrogen bond geometries and protonation states of these groups. It is shown that absence of such an isotope effect is not only compatible with an isolated carboxylate group but also with the presence of a short and strong hydrogen bond.

Introduction

Low-temperature NMR spectroscopy using liquefied gases as solvents has revealed novel possibilities in the study of hydrogen-bonded systems.[1] The slow proton and hydrogen bond exchange regime can often be reached in the temperature range between 100 and 150 K, which allows one to resolve the fine structure of NMR lines attributed to nuclei of intermolecular hydrogen bonds. Under these conditions, the chemical shifts, scalar spin−spin couplings of nuclei involved in a hydrogen

[†] Freie Universität Berlin.
[‡] St. Petersburg State University.

(1) (a) Golubev, N. S.; Denisov, G. S. *J. Mol. Struct.* **1992**, *270*, 263. (b) Golubev, N. S.; Smirnov, S. N.; Gindin, V. A.; Denisov, G. S.; Benedict, H.; Limbach, H. H. *J. Am. Chem. Soc.* **1994**, *116*, 12055. (c) Smirnov, S. N.; Golubev, N. S.; Denisov, G. S.; Benedict, H.; Schah-Mohammedi, P.; Limbach, H. H. *J. Am. Chem. Soc.* **1996**, *118*, 4094. (d) Shenderovich, I. G.; Smirnov, S. N.; Denisov, G. S.; Gindin, V. A.; Golubev, N. S.; Dunger, A.; Reibke, R.; Kirpekar, S.; Malkina, O. L.; Limbach, H. H. *Ber. Bunsen-Ges. Phys. Chem.* **1998**, *102*, 422.

10.1021/ja039280j CCC: $27.50

Chart 1. Structure of the Acetic and Chloroacetic Acid Cyclic Dimers and Acetic Acid Homoconjugate Anions

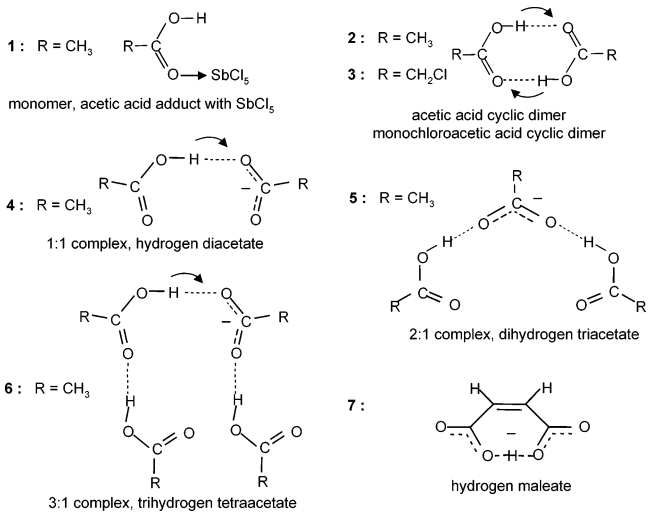

bridge, and isotope effects on these values can provide useful information about the hydrogen bond geometries and dynamics.[2] Isotopic splittings of one signal into several lines arising from partial H/D replacement in mobile proton sites of hydrogen-bonded complexes containing two or more hydrogen bonds can also be detected.[2b] These splittings allow one to establish the composition of H-bonded associates, in particular, the number, *n*, of proton donor molecules AH in hydrogen-bonded clusters $(AH)_n$.[3] They also indicate the extent of mutual influence of neighboring hydrogen bonds, which might be cooperative or anticooperative.[2b,4] Finally, the dielectric constant of liquefied Freon mixtures such as CDF_3/CDF_2Cl strongly increases at low temperatures, giving information about the effects of the solvent polarity and ordering on hydrogen-bonded systems.[5]

The goal of the present study was to apply the above technique to explore various hydrogen-bonded situations of acetic and monochloroacetic acids as models for side-chain interactions of glutamic and aspartic acids in proteins. Thus, we looked for the hydrogen-bonded states depicted in Chart 1. As it is impossible to monitor monomeric carboxylic acids in organic solvents at very low temperatures in the slow hydrogen bond exchange regime because of the high tendency to form cyclic dimers, we choose **1** as a model for monomeric acetic acid. For formic acid, the $SbCl_5$ has been shown previously[6] to break up the cyclic dimer to give $Cl_5Sb \leftarrow O{=}CHOH$, where the C=O group is no longer able to act as proton acceptor even at low temperatures. Novel information was obtained for the cyclic hydrogen-bonded dimers **2** and **3**; these species have been studied previously in the gas phase,[7] in condensed phase, and in solutions.[8] In the bulk liquid state, the structure of acetic acid corresponds to a mixture of cyclic dimers and various hydrogen-bonded clustered chains found in the crystalline state.[9,13a] In addition, complexes of acids with organic bases[1c,10] and with alcohols[11] have been studied using various NMR methods. Although these species have been studied for a long time, they still attract attention of both theoretical[12] and experimental chemists.[13]

Complexes of carboxylic acids with their conjugate bases are of special importance, as they represent the limiting case of the strongest hydrogen bonding.[14] We were interested in these motifs as they occur in cofactors of proteins[15] and enzymes.[16] Recently, we have described using low-temperature NMR the homoconjugated complex **4** of acetic acid with acetate.[2b] Here, we describe in addition the novel complexes **5** and **6** where two and three acetic acid molecules are bound to acetate and compare them with the structure of tetrabutylammonium (TBA) hydrogen maleate **7**.[2b]

To explore the impact of these low-temperature studies for protein NMR, we have also studied as a reference the effect of replacing H_2O by D_2O on the ^{13}C chemical shifts of acetic acid and of acetate in water. To our knowledge, such data have not been reported yet in the literature. Our comparative experiments using aqueous and aprotic polar solvents will explain the unexpected ^{13}C chemical shifts of carboxyl groups in the active site of HIV protease after inhibitor binding found by Smith et al.[17] We will show that the active site of the protein does not correspond to the aqueous but to the aprotic polar environment modeled by solvents such as the Freon mixtures used in this study. Our work will also be of use for the theoretical treatment of hydrogen bonding in the active site of HIV protease studied by Piana[18] et al. and by Northrop.[16c]

We were also interested in scalar spin couplings of the $^{13}COO^1H$ group, which have been inaccessible to date, the

(2) (a) Benedict, H.; Shenderovich, I. G.; Malkina, O. L.; Malkin, V. G.; Denisov, G. S.; Golubev, N. S.; Limbach, H. H. *J. Am. Chem. Soc.* **2000**, *122*, 1979. (b) Schah-Mohammedi, P.; Shenderovich, I. G.; Detering, C.; Limbach, H. H.; Tolstoy, P. M.; Smirnov, S. N.; Denisov, G. S.; Golubev, N. S. *J. Am. Chem. Soc.* **2000**, *122*, 12878. (c) Hansen, P. E. *Prog. NMR Spectrosc.* **1988**, *20*, 207.
(3) Detering, C.; Tolstoy, P. M.; Golubev, N. S.; Denisov, G. S.; Limbach, H. H. *Dokl. RAN* **2001**, *379*, 353; (Engl. ed.) *Dokl. Phys. Chem.* **2001**, *379*, 191.
(4) (a) Golubev, N. S.; Smirnov, S. N.; Schah-Mohammedi, P.; Shenderovich, I. G.; Denisov, G. S.; Gindin, V. A.; Limbach, H. H. *Zh. Obsh. Khim.* **1997**, *67*, 1050; (Engl. ed.) *Russ. J. Gen. Chem.* **1997**, *67*, 1082. (b) Shenderovich I. G.; Limbach H. H.; Smirnov, S. N.; Tolstoy, P. M.; Denisov, G. S.; Golubev, N. S. *Phys. Chem. Chem. Phys.* **2002**, *4*, 5488.
(5) (a) Golubev, N. S.; Denisov, G. S.; Smirnov, S. N.; Shchepkin, D. N.; Limbach, H. H. *Z. Phys. Chem.* **1996**, *196*, 73. (b) Shenderovich, I. G.; Burtsev, A. P.; Denisov, G. S.; Golubev, N. S.; Limbach, H. H. *Magn. Reson. Chem.* **2001**, *39*, S91.
(6) Golubev, N. S.; Kuvatov, A. *Khim. Phys.* **1984**, *3*, 55; (Engl. ed.) *Sov. J. Chem. Phys.* **1985**, *3*, 84.
(7) (a) Almenningen, A.; Bastiansen, O.; Motzfeldt, T. *Acta Chem. Scand.* **1969**, *23*, 2848. (b) Almenningen, A.; Bastiansen, O.; Motzfeldt, T. *Acta Chem. Scand.* **1970** *24*, 747. (c) Derissen, J. L. *J. Mol. Struct.* **1971**, *7*, 67 and 81.
(8) (a) Leiserowitz, L. *Acta Crystallogr.* **1976**, *B32*, 775. (b) Kanters, J. A.; Roelofsen, G. *Acta Crystallogr.* **1976**, *B32*, 3328. (c) Kanters, J. A.; Roelofsen, G.; Feenstra, T. *Acta Crystallogr.* **1976**, *B32*, 3331. (d) Heyne, K.; Huse, N.; Nibbering, E. T. J.; Elsaesser, T. *Chem. Phys. Lett.* **2003**, *369*, 591.
(9) Génin, F.; Quilès, F.; Burneau, A. *Phys. Chem. Chem. Phys.* **2001**, *3*, 932.
(10) (a) Gerritzen, D.; Limbach, H. H. *J. Phys. Chem.* **1980**, *84*, 799. (b) Gerritzen, D.; Limbach, H. H. *J. Am. Chem. Soc.* **1984**, *106*, 869.
(11) Pushkareva, E. G.; Golubev, N. S.; Denisov, G. S. *J. Mol. Liq.* **1983**, *26*, 169.
(12) (a) Payne, R. S.; Roberts, R. J.; Rowe, R. C.; Docherty, R. *J. Comput. Chem.* **1998**, *19*, 1. (b) Nakabayashi, T.; Sato, H.; Hirata, F.; Nishi N. *J. Phys. Chem. A* **2001**, *105*, 245. (c) Lii, J.-H. *J. Phys. Chem. A* **2002**, *106*, 8667. (d) Aquino, A. J. A.; Tunega, D.; Haberhauer, G.; Gerzabek, M. H.; Lischka, H. *J. Phys. Chem. A* **2002**, *106*, 1862.
(13) (a) Nakabayashi, T.; Kosugi, K.; Nishi, N. *J. Phys. Chem. A* **1999**, *103*, 8595. (b) Seifert, G.; Patzlaff, T.; Graener, H. *Chem. Phys. Lett.* **2001**, *333*, 248. (c) Hintze, P. E.; Aloisio, S.; Vaida, V. *Chem. Phys. Lett.* **2001**, *343*, 159.
(14) (a) Kumar, G. A.; Pan, Y.; Smallwood, C. J.; McAllister, M. A. *J. Comput. Chem.* **1998**, *19*, 1345. (b) Brueck, A.; McCoy, L. J.; Kilway, K. V. *Org. Lett.* **2000**, *2*, 2007. (c) Harmon, K. M.; Shaw, K. E.; Sadeki, S. M. *J. Mol. Struct.* **2000**, *526*, 191. (d) Barczynski, P.; Kowalczyk, I.; Grundwald-Wyspianska, M.; Szafran, M. *J. Mol. Struct.* **1999**, *484*, 117. (e) Perrin, C. L.; Nielson, J. B. *J. Am. Chem. Soc.* **1997**, *119*, 12734.
(15) Luecke, H.; Schobert, B.; Richter, H. T.; Cartailler, J. P.; Lanyi, J. K. *J. Mol. Biol.* **1999**, *291*, 899.
(16) (a) Mildvan, A. S.; Massiah, M. A.; Harris, T. K.; Marks, G. T.; Harrison, D. H. T.; Viragh, C.; Reddy, P. M.; Kovach, I. M. *J. Mol. Struct.* **2002**, *615*, 163. (b) Coates, L.; Erskine, P. T.; Crump, M. P.; Wood, S. P.; Cooper, J. B. *J. Mol. Biol.* **2002**, *318*, 1405. (c) Northrop, D. B. *Acc. Chem. Res.* **2001**, *34*, 790.
(17) Smith, R.; Brereton, I. M.; Chai, R. Y.; Kent, S. B. H. *Nat. Struct. Biol.* **1996**, *3*, 946.

hydrogen bond proton chemical shifts in relation to the hydrogen bond geometries, how the latter are affected by deuteration of a given hydrogen bond site and of a neighboring site—which provides information about the mutual coupling of two hydrogen bonds, and whether these phenomena can also be observed by ^{13}C NMR of the carboxyl groups. In addition, we were interested to learn something about the internal fluxionality of the complexes **5** and **6**, which imply a fast internal exchange of the acid molecules with the conjugate anion. We came across such rearrangements in our previous study of the acetic acid/pyridine 3:1 complex,[1c] corresponding to **5** hydrogen bonded to pyridinium, as well as in complexes of several HF molecules with fluoride.[4b]

The paper is organized as follows. After an Experimental Section, the results of our multinuclear NMR experiments of acetic and monochloroacetic acids and their deuterated analogues without and in the presence of tetrabutylammonium salts in the low-freezing Freon mixture CDF_3/CDF_2Cl, and of acetic acid in H_2O and D_2O are presented and discussed. In the discussion, the hydrogen bond geometry—chemical shift correlation method will be used to establish the geometry of the hydrogen bonds, as well as geometric isotope effects, and how these effects can be observed by ^{13}C NMR. Finally, effects of cooperativity in the systems with two or more hydrogen bonds will be discussed.

Experimental Section

The experimental low-temperature technique used for the present investigation has been described in detail elsewhere.[5b] The Bruker AMX-500 NMR spectrometer used was equipped with a low-temperature probe head, which allowed us to perform experiments down to 100 K. ^2H NMR spectra were measured without lock. Commercially available acetic acid-1-^{13}C (99% enrichment, Deutero GmbH) was employed for the experiments. Chloroacetic acid-1-^{13}C was prepared by direct chlorination of acetic acid-1-^{13}C in the presence of $SbCl_5$ (Aldrich) as catalyst[19] and purified by repeated sublimation under reduced pressure. Tetrabutylammonium acetate (TBA acetate) was prepared by mixing acetic acid with 1 M methanol solution of TBA hydroxide and subsequent removal of methanol and water formed in this reaction by azeotropic distillation with dichloromethane. Chemicals were weighed and placed into thick-walled sample NMR tubes equipped with PTFE valves (Wilmad, Buena). The solvent mixture $CDF_3/CDClF_2$ for the low-temperature NMR experiments was prepared by a modified recipe proposed by Siegel and Anet.[20] During the synthesis, it is difficult to control conditions precisely in order to get the mixture of a given composition, so from synthesis to synthesis the solvent composition varied between 15:1 and 2:1, estimated from the intensity of the residual ^1H NMR solvent signals. However, the actual values obtained during such estimations might be affected by the possible exchange of CDF_3 and CDF_2Cl deuterons with protons of residual water molecules during the synthesis, thus resulting in the descrepancy between CHF_3/CHF_2Cl and CDF_3/CDF_2Cl ratios. Within this range, the solvent freezing point and the solubility of studied acetic acid complexes stayed sufficient to perform the low-temperature measurements. Solvent was added to the sample tubes by vacuum transfer. Acetic acid was deuterated by passing gaseous DCl, produced from 96% D_2SO_4 (99.5% D, Deutero GmbH) with dry solid NaCl, through a solution of acetic acid in CH_2Cl_2. Chloroacetic acid was deuterated in the COOH site by repeatedly dissolving the compound in CH_3OD and removing the solvent in vacuo. The total deuterium fraction was determined by NMR, in particular, by comparison of the integrated signal intensity of the residual mobile proton site with those of the immobile CH protons. ^1H, ^2H, and ^{13}C NMR chemical shifts were measured using fluoroform, CHF_3 (CDF_3), as internal standard, and were converted to the conventional TMS scale. The approximate overall acid concentration of the samples, estimated by weighing acetic acid and measuring the volume of the solution at low temperatures (~120 K), was ~0.02 M.

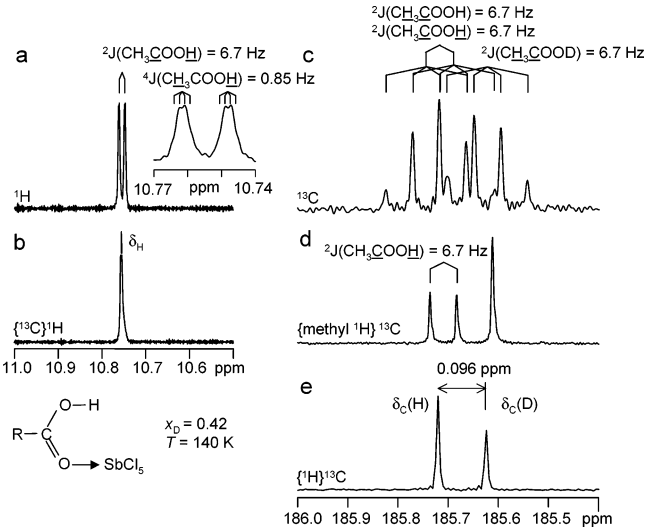

Figure 1. Partial NMR spectra of acetic acid-1-^{13}C enriched in the carboxyl position in the presence of a 2-fold excess of $SbCl_5$ dissolved in CDF_3/CDF_2Cl (2:1) at 140 K. x_D is the deuterium fraction of the carboxyl group. ^1H Larmor frequency, 500.13 MHz. ^1H signal of the hydroxyl group without (a) and with (b) $\{^{13}C\}$ decoupling. ^{13}C signal of the carboxyl group (c) without decoupling, (d) with selective decoupling of the methyl protons, and (e) with broad-band $\{^1H\}$ decoupling.

Results

Adduct of Monomeric Acetic Acid with $SbCl_5$ (1). In Figure 1 are depicted partial ^1H and ^{13}C spectra of partially deuterated ^{13}C-enriched acetic acid dissolved in CDF_3/CDF_2Cl (2:1) in the presence of a 2-fold excess of $SbCl_5$. The deuterium fraction in the mobile proton site was $x_D = 0.42$, and the sample temperature 140 K. The carboxylic proton signal resonates at 10.754 ppm. It is split into a doublet arising from scalar spin—spin coupling with the carboxylic carbon nucleus, with $^2J(CH_3COOH) = 6.7$ Hz. This assignment is supported by ^{13}C-decoupling (Figure 1b). Each component of the doublet is furthermore split into a barely resolved quartet, arising from long-range scalar coupling with the methyl group protons, where $^4J(CH_3COOH) \approx 0.85$ Hz. Partial H/D replacement does not affect the shape of the proton signal.

In the $\{^1H\}$-decoupled ^{13}C NMR spectrum (Figure 1e), two lines are observed at $\delta_C(H) = 185.721$ ppm for the protonated species and at $\delta_C(D) = 185.625$ ppm for the deuterated species. Selective decoupling of the methyl protons produces a doublet splitting for the protonated species (Figure 1d), with $^2J(CH_3COOH) = 6.7$ Hz. Finally, in the uncoupled ^{13}C spectrum (Figure 1c), all signals are split further into quartets, where $^2J(CH_3COOD) = 6.7$ Hz, by chance equal to $^2J(CH_3COOH)$, within the margin of experimental error. All NMR parameters are assembled in Table 1.

Cyclic Dimers of Acetic (2) and of Monochloroacetic Acid (3). The low-temperature ^1H, ^2H, and ^{13}C NMR signals of the carboxyl group of partially deuterated in OH group acetic acid-1-^{13}C dissolved in CDF_3/CDF_2Cl (4:1) are depicted in Figure 2. As will be shown in the following, these signals correspond

(18) Piana, S.; Sebastiani, D.; Carloni, P.; Parrinello, M. *J. Am. Chem. Soc.* **2001**, *123*, 8730.
(19) Becker, H. G. O. *Organikum*; Barth: Leipzig, 1993; p 170.
(20) Siegel, J. S.; Anet, F. A. L. *J. Org. Chem.* **1988**, *53*, 2629.

Table 1. NMR Parameters of Two Isotopologues of Acetic Acid Complex with $SbCl_5$ (**1**) in a Freon Mixture at 140 K[a]

	1, $CH_3COOL{\cdot}SbCl_5$
$\delta_H \pm 0.005$/ppm	10.754
$\delta_C(H) \pm 0.005$/ppm	185.721
$\delta_C(D) \pm 0.005$/ppm	185.625
$\delta_C(D) - \delta_C(H) \pm 0.007$/ppm	−0.096
$^4J(CH_3COOH) \pm 0.2$/Hz	0.85
$^2J(CH_3COOH) \pm 0.2$/Hz	6.7
$^2J(CH_3COOH) \pm 0.2$/Hz	6.7
$^2J(CH_3COOD) \pm 0.2$ /Hz	6.7

[a] ^{13}C Chemical shifts correspond to carboxylic carbon. L = H, D.

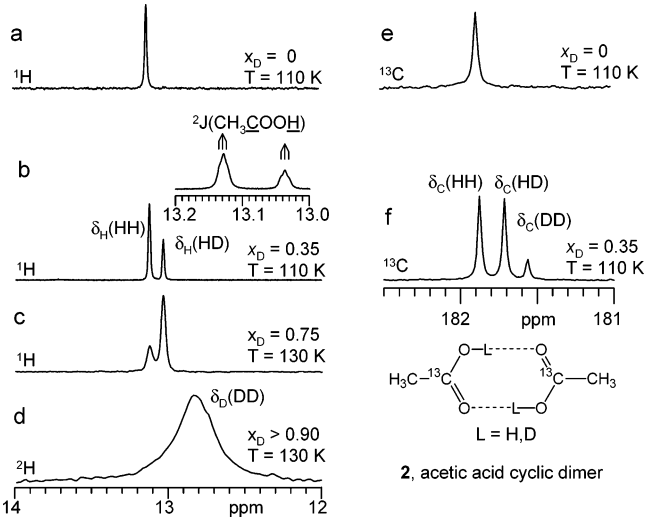

Figure 2. ^1H, ^2H, and $\{^1H\}^{13}C$ NMR signals of the carboxyl group of acetic acid-1-^{13}C dissolved in CDF_3/CDF_2Cl (4:1) obtained at 110 K as a function of the deuterium fraction x_D in the mobile proton site. (d) was obtained in CHF_3/CHF_2Cl solution.

Table 2. NMR Parameters of Three Isotopologues of Acetic (CH_3COOL, **2**) and Chloroacetic ($CClH_2COOL$, **3**) Acid Cyclic Dimers in a Freon Mixture at 110 K. L = H, D

	2, $(CH_3$-$^{13}COOL)_2$	**3**, $(CClH_2$-$^{13}COOL)_2$
$\delta_H(HH) \pm 0.005$/ppm	13.127	13.250
$\delta_H(HD) \pm 0.005$/ppm	13.035	13.165
$\delta_H(HD) - \delta_H(HH) \pm 0.007$/ppm	−0.092	−0.085
$\delta_D(HD) \pm 0.03$/ppm	12.92[a]	
$\delta_D(DD) \pm 0.03$/ppm	12.83	
$\delta_D(DD) - \delta_D(HD) \pm 0.04$/ppm	−0.09[a]	
$\delta_D(DD) - \delta_H(HH) \pm 0.03$/ppm	−0.30	
$\delta_C(HH) \pm 0.005$/ppm	181.874	176.693
$\delta_C(HD) \pm 0.005$/ppm	181.713	176.551
$\delta_C(DD) \pm 0.005$/ppm	181.561	176.417
$\delta_C(HD) - \delta_C(HH) \pm 0.008$/ppm	−0.161	−0.142
$\delta_C(DD) - \delta_C(HD) \pm 0.008$/ppm	−0.152	−0.134
$^2J(CH_3COOH)$ (in HH form) ± 0.5/Hz	3.0	3.0
$^2J(CH_3COOH)$ (in HD form) ± 0.5/Hz	3.0	3.0

[a] Calculated on the basis of sum rule, proposed in (4b).

to the cyclic dimer. The chemical shifts are then labeled as $\delta_X(LL)$, where X represents the nucleus observed and LL = HH, HD, and DD, the three isotopologues of the dimer. The NMR parameters obtained are assembled in Table 2.

At a deuterium fraction of $x_D = 0$, a single carboxylic proton signal is observed in the ^1H NMR spectrum at $\delta_H(HH) = 13.127$ ppm (Figure 2a). The corresponding ^{13}C signal appears at $\delta_C(HH) = 181.874$ ppm (Figure 2e). These chemical shifts are

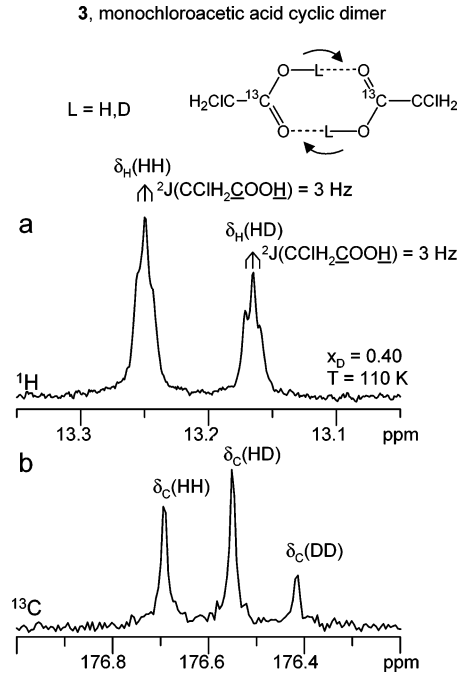

Figure 3. ^1H (a) and $\{^1H\}^{13}C$ (b) NMR spectra of 1-^{13}C-labeled chloroacetic acid in CDF_3/CDF_2Cl (4:1) at 110 K and $x_D = 0.4$.

not affected by moderate changes of the acid concentration. The spectra of partially deuterated samples exhibit additional lines, arising from the different isotopologues. In the ^1H NMR spectrum, one additional line is observed at $\delta_H(HD) = 13.035$ ppm, assigned to the HD isotopologue (Figure 2b,c). The intensity of this line increases with an increasing deuterium fraction as expected. The ^{13}C NMR spectra exhibit two additional lines, characterized by the chemical shifts $\delta_C(HD) = 181.713$ ppm and $\delta_C(DD) = 181.561$ ppm (Figure 2f).

We note that the proton signals of the HH and the HD isotopologues are split into a barely resolved triplets (see inset of Figure 2b); as this splitting is not observed in corresponding samples of non-^{13}C-enriched acetic acid, we assign it to the coupling of the hydrogen bond protons with the two ^{13}C atoms of the enriched dimer, characterized by the coupling constant $^2J(CH_3COOH) \approx 3.0$ Hz.

Finally, in Figure 2d is depicted the low-temperature ^2H NMR spectrum of acetic acid dissolved in CHF_3/CHF_2Cl, at a deuteron fraction of $x_D > 0.9$. The signal stems dominantly from the doubly deuterated cyclic dimer and, to a small extent, from the half-deuterated dimer. The signal is broadened because of ^2H quadrupolar relaxation and magnetic field fluctuations, as the spectra were acquired without magnetic field lock. The resulting field instability precluded longer acquisition times necessary to measure the chemical shift of the HD species at lower deuterium fractions x_D. Nevertheless, a substantial upfield shift $\delta_D(DD) - \delta_H(HH) = -0.30$ ppm is observed.

In Figure 3 are depicted the ^1H and ^{13}C NMR signals of chloroacetic acid-^{13}C, at a deuterium fraction of $x_D = 0.4$; the NMR parameters obtained are included in Table 2. The spectral patterns are similar to those for the acetic acid dimer. However, the signals are sharper and the $^1H-^{13}C$ coupling is better resolved as compared to the case of acetic acid, although the value of $^2J(CH_3COOH) \approx 3.0$ Hz is the same.

Acetic Acid Anion. We tried to measure the ^{13}C NMR spectrum of free acetate by preparing the sample containing

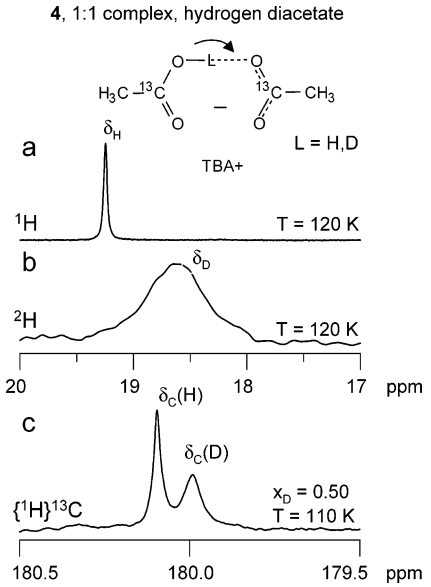

Figure 4. Low-temperature ^{1}H (a), ^{2}H (b), and {^{1}H}^{13}C (c) NMR spectra of a sample containing 0.02 M partially deuterated ^{13}C-labeled acetic acid ($x_D = 0.5$) and 0.02 M TBA acetate ^{13}C-labeled in the carboxylate group (15:1 CDF_3/CDF_2Cl). Adapted from ref 2b.

0.02 M tetrabutylammonium acetate (TBA^+ $^{13}COO^-$), but unfortunately, we were unable to get any ^{13}C signal at low temperature in the region of carboxylic carbon signals. This is probably due to the interaction of such acetate anions with the surface OH groups, present on the walls of glass sample tube.

The 1:1 Complex of Acetic Acid with Its Conjugate Base (Hydrogen Diacetate 4). Typical ^{1}H, ^{2}H, and ^{13}C signals of the 1:1 complex **4** of $CH_3{}^{13}COOH$ with its conjugate base $CH_3{}^{13}COO^-$ using TBA as the countercation are depicted in Figure 4. The composition of the solvent mixture CDF_3/CDF_2Cl was ~15:1, as measured from the ^{1}H spectrum. These spectra have been published in a preliminary communication;[2b] they are included here for comparison with the other novel complexes **5** and **6** described below.

The proton signal of **4** resonates at $\delta_H(H) = 19.25$ ppm and exhibits a negative value of the primary isotope effect $\delta_D(D) - \delta_H(H) = -0.6$ ppm. The H/D isotope effect of -0.20 ppm on the carboxylic carbon nuclei is also negative, as in all other cases presented above (Table 3).

The 2:1 Complex of Acetic Acid with Its Conjugate Base (Dihydrogen Triacetate 5). The addition of another acetic acid molecule to **4** leads to a new species, which will be shown to correspond to a 2:1 acetic acid−acetate complex, dihydrogen triacetate **5**, exhibiting two hydrogen bonds. A single line is observed for the HH species at $\delta_H(HH) = 16.39$ ppm (Figure 5). After partial H/D substitution ($x_D = 0.7$), a new signal appears for the HD species at $\delta_H(HD) = 16.68$ ppm, corresponding to a positive vicinal isotope effect. The corresponding ^{2}H NMR signal is very broad, the signals of the partially deuterated and the fully deuterated complexes could not be resolved.

In Figure 6 are depicted the ^{1}H and ^{13}C NMR spectra of a partially deuterated sample, where **4** and **5** are of a comparable concentration, exhibiting a deuterium fraction of $x_D = 0.25$. All signals shift slightly to low field with decreasing temperature as expected for asymmetric hydrogen-bonded systems.[5a] At high temperatures, the onset of proton and hydrogen bond exchange

Table 3. NMR Parameters of Isotopologues of Acetic Acid Complexes with Acetate Anion, with TBA Counterion

	4, 1:1 complex hydrogen diacetate	**5**, 2:1 complex dihydrogen triacetate	**6**, 3:1 complex trihydrogen tetraacetate
$\delta_H \pm 0.01$/ppm	19.25		
$\delta_D \pm 0.03$/ppm	18.63		
$\delta_D - \delta_H \pm 0.03$/ppm	−0.62		
$\delta_C(H) \pm 0.01$/ppm	180.19		
$\delta_C(D) \pm 0.01$/ppm	179.99		
$\delta_C(D) - \delta_C(H) \pm 0.015$/ppm	−0.20		
$\delta_H(HH) \pm 0.01$/ppm		16.39	
$\delta_H(HD) \pm 0.01$/ppm		16.68	
$\delta_D(HD+DD) \pm 0.1$/ppm		16.08	
$\delta_H(HD) - \delta_H(HH) \pm 0.02$/ppm		0.29	
$\delta_C(HH) \pm 0.01$/ppm		179.39	
$\delta_C(HD) \pm 0.01$/ppm		179.27	
$\delta_C(DD) \pm 0.01$/ppm		179.14	
$\delta_C(HD) - \delta_C(HH) \pm 0.015$/ppm		−0.12	
$\delta_C(DD) - \delta_C(HD) \pm 0.015$/ppm		−0.13	
$\delta_H(HHH) \pm 0.02$/ppm			14.76
$\delta_H(HHD) \pm 0.02$/ppm			14.87
$\delta_H(HDD) \pm 0.02$/ppm			14.99
$\delta_H(HHD) - \delta_H(HHH) \pm 0.03$/ppm			0.11
$\delta_H(HDD) - \delta_H(HHD) \pm 0.03$/ppm			0.12

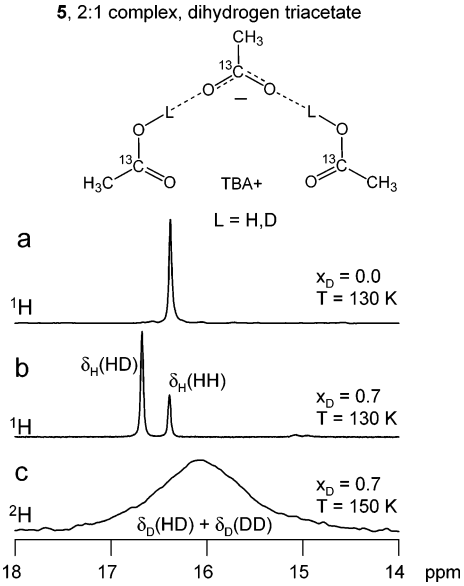

Figure 5. Low-temperature ^{1}H and ^{2}H NMR spectra of dihydrogen triacetate (15:1 CDF_3/CDF_2Cl). (a) ^{1}H NMR spectrum of the sample containing no deuterium; (b, c) ^{1}H and ^{2}H NMR spectra of the sample containing 70% of deuterium in the mobile proton sites ($x_D = 0.7$).

leads to line broadening, but at 130 K, all lines are sharp. At lower temperatures, all lines exhibit the usual line broadening arising from the increase of the solvent viscosity. No major spectral changes are observed for the ^{1}H signals of **4** and **5** and for the ^{13}C signals of **4**. By contrast, the high-field carboxyl ^{13}C signal exhibits very interesting changes. Around 130 K, a signal trio is observed, assigned to the three isotopologues of **5**, where $\delta_C(HH) = 179.39$ ppm, $\delta_C(HD) = 179.27$ ppm, and $\delta_C(DD) = 179.14$ ppm. No other ^{13}C signal could be observed for **5**, indicating that all carbon atoms of **5** are chemically equivalent within the NMR time scale. These signals broaden, however, below 130 K much more than the ^{13}C signal of **4**, indicating that a fast chemical exchange is taking place at 130

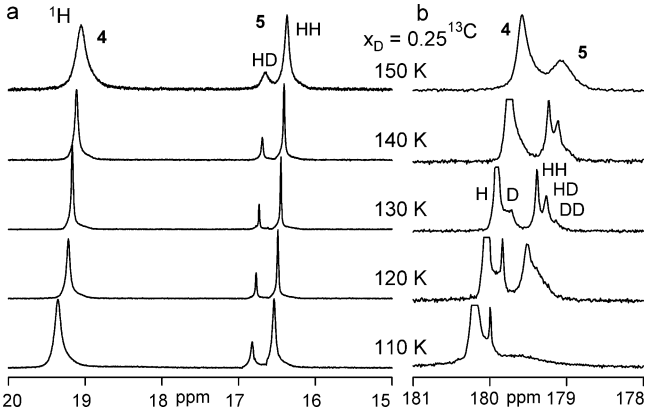

Figure 6. Temperature dependence of the low-field ^{1}H (a) and carboxylic carbon ^{13}C NMR signals (b) of dihydrogen triacetate of a sample with a deuterium fraction in the mobile proton sites of $x_D = 0.25$ (15:1 CDF_3/CDF_2Cl).

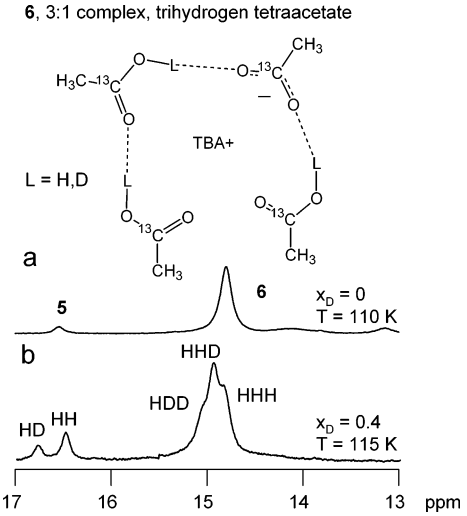

Figure 7. Low-temperature ^{1}H NMR spectra of trihydrogen tetraacetate (2:1 CDF_3/CDF_2Cl); (a) ^{1}H NMR spectrum of the sample containing no deuterium; (b) ^{1}H NMR spectrum of the sample containing 40% deuterium ($x_D = 0.4$).

K that becomes slower below this temperature. Unfortunately, the slow exchange regime could not be reached.

The 3:1 Complex of Acetic Acid with Its Conjugate Base (Trihydrogen Tetraacetate 6). Finally, another novel complex **6** could be observed after further addition of acetic acid, exhibiting a strong high-field ^{1}H NMR signal as illustrated in Figure 7. Partial deuteration reveals three isotopologues at $x_D = 0.4$, where δ_H(HHH) = 14.76 ppm, δ_H(HHD) = 14.87 ppm, and δ_H(HDD) = 14.99 ppm (Table 3). Unfortunately, we were unable to obtain ^{2}H and ^{13}C signals of this species.

H/D Isotope Effects on the Carboxylic Carbon NMR Chemical Shifts of Acetic Acid and Acetate in Water and Chloroform at Room Temperature. The question arises whether the data obtained for carboxylic carbon chemical shift in Freon solution at low temperatures are consistent with the measurements in water solutions. In Figure 8, we show the carboxylic acid/carboxylate ^{13}C signals of ^{13}C-enriched acetic acid dissolved in H_2O and D_2O at a concentration of 0.006 M and pH 13.6 (Figure 8a) as well as pH 1.3 (Figure 8b). The pH values were adjusted by adding KOH/KOD or H_2SO_4/D_2SO_4. The results are assembled in Table 4.

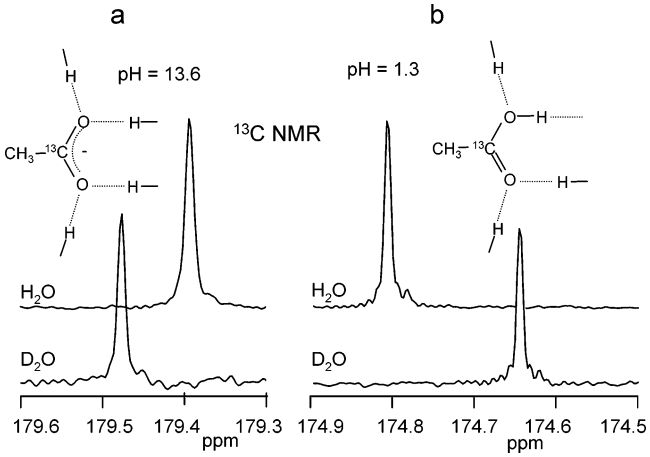

Figure 8. H/D isotope effect on carboxylic ^{13}C NMR chemical shift of 0.006 M acetic acid in water at high pH and at low pH at 298 K.

We note positive ionization shifts, i.e., a low-field shift of the carboxylic carbon signal when the carboxyl group is converted into a carboxylate group. When H is replaced by D, the carboxylate signal shifts to low field; i.e., one observes a positive H/D isotope effect on the ^{13}C chemical shift, whereas a negative effect is observed for the carboxyl group. Thus, the pH dependence of the carbon isotope shift should be described by the following equation

$$\Delta\delta^{13}C(D_2O) = \frac{-0.159}{1+10^{pH-pK_a}} + \frac{0.082}{1+10^{pK_a-pH}} \qquad (1)$$

From this equation, we expect a vanishing isotope effect around pH 5.

To elucidate the effect of the solvent on the ionization shifts, we prepared a series of samples where we added increasing amounts of tetrabutylammonium hydroxide to 0.02 M solutions of acetic acid, using in the first series pure water with a deuterium fraction $x_D = 0.1$ as solvent and in the second series $CDCl_3$. In the case of the chloroform samples, the water produced was removed by azeotropic distillation. However, no particular attempts were made to prepare completely water-free samples.

The ^{13}C chemical shifts obtained for the carboxylic/carboxylate carbons are plotted in Figure 9 as a function of the tetrabutylammonium hydroxide/acid ratio. The solid lines are guides for the eye and are not the results of a quantitative analysis. The results will be interpreted in detail below.

Discussion

In this section, we will first discuss the structures of the species observed as well as their NMR parameters such as chemical shifts, spin−spin couplings, and H/D isotope effects on the chemical shifts. Then we will correlate the ^{1}H NMR chemical shifts with the H-bond geometries. Finally, we will address the effects of cooperativity in the systems with two (or more) coupled hydrogen bonds.

Adduct of Monomeric Acetic Acid with $SbCl_5$ (1). We assign the chemical structure depicted in Figure 1 to the adduct **1** of $CH_3{}^{13}COOH$ with the Lewis acid $SbCl_5$, where the C═O group of acetic acid is coordinated to Sb. A scalar coupling of the type $^2J(COOH)$ has been observed here for the first time to our knowledge. We expect a similar value for the true monomer

Table 4. Carboxylic Chemical Shifts (in ppm) of $CH_3{}^{13}COOH$ and $CH_3{}^{13}COO^-$ at 298 K and 0.006 M in H_2O (D_2O) and $CDCl_3$

chemical shift COOH in H_2O	$\delta^{13}COOH{\cdot}H_2O$	174.81
chemical shift COOD in D_2O	$\delta^{13}COOD{\cdot}D_2O$	174.65
chemical shift COO^- in H_2O	$\delta^{13}COO^-{\cdot}H_2O$	179.40
chemical shift COO^- in D_2O	$\delta^{13}COO^-{\cdot}D_2O$	179.48
chemical shift COOH in $CDCl_3$	$\delta^{13}COOH{\cdot}CDCl_3$	176.2
chemical shift COO^- in $CDCl_3$	$\delta^{13}COO^-{\cdot}CDCl_3$	173.5
ionization shift in H_2O	$\delta^{13}COO^-{\cdot}H_2O - \delta^{13}COOH{\cdot}H_2O$	4.59
ionization shift in D_2O	$\delta^{13}COO^-{\cdot}D_2O - \delta^{13}COOD{\cdot}D_2O$	4.83
ionization shift in $CDCl_3$	$\delta^{13}COO^-{\cdot}CDCl_3 - \delta^{13}COOH{\cdot}CDCl_3$	−2.7
solvent isotope shift COOL	$\delta^{13}COOD{\cdot}D_2O$ -$\delta^{13}COOH{\cdot}H_2O$	−0.16
solvent isotope shift COO^-	$\delta^{13}COO^-{\cdot}D_2O$ -$\delta^{13}COO^-{\cdot}H_2O$	+0.08

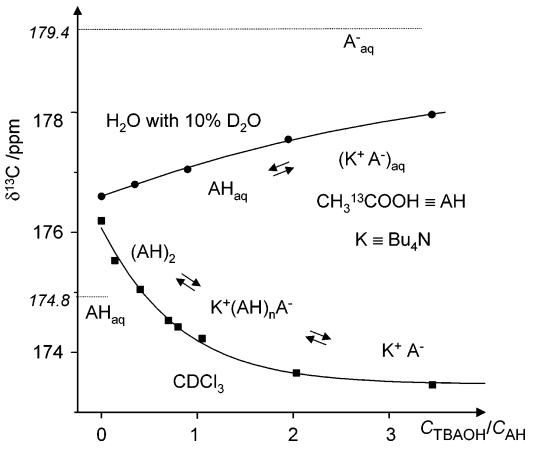

Figure 9. Acetic acid carboxylic carbon ^{13}C NMR chemical shift as a function of the amount of added TBAOH measured in a H_2O/D_2O mixture and in $CDCl_3$ at room temperature (concentration of acid was 0.02 M).

of acetic acid for which **1** is currently the best available model. Previously, only scalar spin couplings of carboxylic protons of the type $^3J(HCOOH)$ have been observed, referring to the cyclic dimer of formic acid, to the 1:1 complex of formic acid with hexamethylphosphoramide,[21] or across hydrogen bonds to the ^{15}N nucleus of pyridine-^{15}N, $^{1h}J(RCOOH...N)$.[1c,5a]

The observation of the coupling $^2J(COOH)$ proves that proton exchange of **1** is slow within the NMR time scale. This means that **1** does not exhibit a tendency to form cyclic dimers in which a fast proton exchange can take place, in contrast to acetic acid. This interpretation is supported by the finding that partial deuteration does not affect the ^1H spectrum at low temperatures, as in the case of acetic acid described below. The deuterated species gives rise to a high field shifted ^{13}C signal, exhibiting an isotope effect of $\delta_C(D) - \delta_C(H) = -0.096$ ppm.

For formic acid monomer, a low-frequency shift of the ν OH band from 3520 to 3450 cm^{-1} has been observed[6] for the adduct with $SbCl_5$ in $CDCl_3$, a finding that has been interpreted in terms of a weak solute−solvent interaction, possibly a weak hydrogen bond. Such a phenomenon is also plausible for **1** in the Freon solvent mixture used.

Because of the different chemical structures of **1** and monomeric acetic acid it is difficult to take the ^1H and ^{13}C chemical shifts of 10.76 and 185.72 ppm of the former as representative values for the latter. Indeed, a value of 5.9 ppm has been reported for the proton chemical shift of acetic acid monomer in CCl_4, but this value may be affected by proton exchange with residual water.[22] Nevertheless, we think that the scalar coupling constants as well as the H/D isotope effect on the ^{13}C chemical shifts of both species are comparable.

Cyclic Dimers of Acetic (2) and of Monochloroacetic Acid (3). The observation of two carboxylic proton signals and three carboxylic carbon signals in partially deuterated samples of acetic acid and chloroacetic acid in the Freon mixture used clearly indicates that the species observed correspond to the HH, HD, and DD isotopologues of the cyclic dimers, which exchange slowly at 110 K within the NMR time scale. The different chemical shifts for the isotopologues arise from anharmonic effects leading to slightly different hydrogen bond geometries. These isotope effects will be discussed in a later section. For a cyclic trimer with three equivalent H-bonds and fast exchanging hydrons, one would expect three proton lines for the HHH, HHD, and HDD isotopologues[3] and four corresponding carbon signals for the HHH, HHD, HDD, and DDD isotopologues.

In some studies of acetic acid associates by IR spectroscopy methods, cyclic dimers have been classified as moderately strong hydrogen-bonded complexes, exhibiting a substantial barrier for the proton motion.[23] For example, in the case of the corresponding benzoic acid dimers, rate constants for the double proton transfer of $\sim 10^{10}$ s^{-1} have been observed around 100 K in the solid state.[24] The observation of a single ^{13}C signal for the HD isotopologues indicates that the double proton transfer in the cyclic dimers is also very fast in solution around 110 K. Otherwise, we would expect two signals for this isotopologue, one for the RCOOH and the other for the RCOOD group.

The relative integrated intensities of the NMR signals of the various isotopologues are also consistent with the assignment given in Figure 2. According to a simple statistical model, the portion of HH, HD, and DD isotopologues in an equilibrium mixture should be equal to $(1 - x_D)^2$, $2x_D(1 - x_D)$, and x_D^2, respectively, where x_D is the total deuterium fraction. The integrated signal intensities found in the ^1H and ^{13}C NMR spectra—within the margin of experimental error—correspond to the statistical values, calculated by assuming the equilibrium constant $K = 4$ for the formation of two HD dimers from a HH and a DD dimer. In particular, for $x_D = 0.35$, the integrated intensities in the ^1H spectrum relate as 1.9:1 and those in the ^{13}C spectrum as 4:4:1, in full accordance with the simple model (Figure 2b,f). In principle, we note that isotopic fractionation could occur leading to a value of K that deviates from the statistical value.

(21) Golubev, N. S.; Denisov, G. S.; Koltsov, A. I. *J. Mol. Struct.* **1981**, *75*, 333.

(22) Jentschura, U.; Lippert, E. *Ber. Bunsen-Ges. Phys. Chem.* **1971**, *75*, 556.
(23) Miura, S.; Tuckerman, M. E.; Klein, M. L. *J. Chem. Phys.* **1998**, *109*, 5290.
(24) (a) Stöckli, A.; Maier, B. H.; Kreis, R.; Meyer, R.; Ernst, R. R. *J. Chem. Phys.* **1990**, *93*, 15002. (b) Horsewill, A. J.; Brougham, D. F.; Jenkinson, R. I.; McGloin, C. J.; Trommsdorff, H. P.; Johnson, M. R. *Ber. Bunsen-Ges. Phys. Chem.* **1998**, *102*, 317. (c) Jenkinson, R. I.; Ikram, A.; Horsewill, A. J.; Trommsdorff, H. P. *Chem. Phys.* **2003**, *294*, 95.

Because of the fast proton tautomerism inside cyclic dimers, the carboxylic protons are coupled to two ^{13}C atoms, in contrast to the adduct with $SbCl_5$. Intermolecular proton exchange would lead to a disappearance of this coupling. This means that the hydrogen bond exchange rate of a dimer is of the order or smaller than the inverse of the coupling constant of $^2J(RCOOH) = 3$ Hz. The observation that this coupling is better resolved for $CH_2Cl^{13}COOH$ than for $CH_3{}^{13}COOH$ indicates slightly faster hydrogen bond exchange rates for the latter. This interpretation is also supported by the sharper ^{13}C signals.

For comparison with the value of $^2J(RCOOH) = 6.7$ Hz measured for **1** we need to multiply the experimental values for the cyclic dimers by a factor of 2, leading to values of 6 Hz. The reduction of 0.7 Hz can be attributed either to the electron-accepting influence of the Lewis acid or to a slight increase of the OH-bond length in the cyclic dimer. A similar effect was found previously for the $^3J(HCOOH)$ coupling constant of formic acid dimer and the adduct of formic acid with $SbCl_5$.[6] Finally, we would like to mention that a value of $^2J(HCOOH) = 10.62$ Hz was calculated for the cyclic dimer of formic acid by Pecul et al.,[25] which compares well with the experimental value of ~6 Hz found in this study.

The 1:1 Complex of Acetic Acid with Its Conjugate Base (Hydrogen Diacetate 4). Within the NMR time scale, the two carboxyl groups of **4** are chemically equivalent. As has been discussed previously,[2b] this finding is consistent with either a single well potential for the proton motion (case a), a symmetric double well exhibiting delocalized hydron states (case b), or a fast conversion of two tautomers, where the hydron motion is coupled to solvent reorientation (case c). The large negative primary effect provides evidence for either case b or c, as case a is expected to give rise to a positive effect.[2b] It is interesting to note that this effect "translates" a large negative secondary isotope effect on the ^{13}C chemical shifts. We note that the line width of the deuteron signal of **4** is larger as compared to the cyclic dimer **2**, although the sample temperatures are comparable. At first sight, one could think that this effect arises from a larger quadrupole coupling constant of **4** as compared to **2** and hence a larger electric field gradient at the ^2H nucleus. However, the OHO hydrogen bond of **4** is stronger and shorter, and the deuteron is more localized in the hydrogen bond center as compared to **2**. Hence, the quadrupole coupling constant should be smaller for **4** than for **2**. Therefore, it is more likely that the larger ^2H line width of **4** arises from a larger correlation time of the anion, which is probably caused by contact with the tetrabutylammonium counterion.

The 2:1 Complex of Acetic Acid with Its Conjugate Base (Dihydrogen Triacetate 5). The ^1H signals of the HH and the HD isotopologues of **5** clearly establish the chemical structure of **5** depicted in Chart 1, with two equivalent hydrogen bonds. By contrast to **2**, the remaining proton is shifted to low field when the other is replaced by a deuteron, which indicates an anticooperative coupling of both hydrogen bonds discussed in more detail below. However, this structure is fluxional and **5** is characterized by a very fast exchange of all carboxylic protons without dissociation of the complex. If the process occurred via a dissociation, the process should be associated with a fast interconversion of all isotopologues of **4** and **5**, which is not the case.

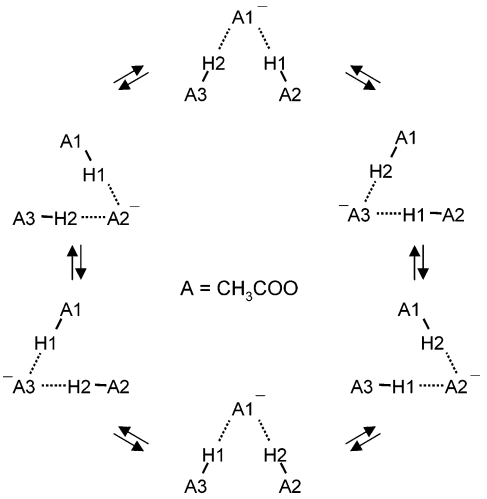

Figure 10. Proposed scheme of the six-step exchange cycle, which makes all three carboxylic carbons in TBA dihydrogen triacetate magnetically equivalent in NMR time scale.

A careful analysis of the process observed leads to a reaction network illustrated in Figure 10, consisting of six elementary steps involving six different species. Each step involves a hydrogen bond jump of a given terminal acetic acid to the other and a dislocation of the proton in the hydrogen bond, which is not broken during the step. Thus, the observed ^{13}C chemical shifts of the three isotopologues of **5** represent averages over the central and the terminal carbon sites. We note that these secondary isotope effects are quite similar to each other, i.e., $\delta_C(HD) - \delta_C(HH) = -0.12$ ppm and $\delta_C(DD) - \delta_C(HD) = -0.13$ ppm. If we had been able to reach the slow hydrogen bond exchange regime, we would have expected three lines for the central carbon sites of the HH, HD, and the DD isotopologues and four lines for the terminal carbon sites of the HH, HD, DH, and DD isotopologues.

We note that we have found previously a related hydrogen bond exchange for the linear 2:1 complex of acetic acid with pyridine,[1c] where the two acetic acid molecules interconvert rapidly at low temperatures, and for the complex of collidinium hydrogen bifluoride.[26]

The 3:1 Complex of Acetic Acid with Its Conjugate Base (Trihydrogen Tetraacetate 6). The three proton signals provide evidence for a complex containing three coupled hydrogen bonds, i.e., a 3:1 complex of acetic acid with acetate as depicted in Chart 1. The puzzle in the beginning of this work was again that for such a structure one would expect separate signals for the terminal and the central hydrogen bond protons. The fact that only a single proton signal is observed, indicates again a fast hydrogen bond exchange process as illustrated in Figure 11. The process is similar to one proposed for the dihydrogen triacetate and consists of 12 elementary steps involving 12 species, which interconvert by a hydrogen bond jump of one terminal acetic acid to the other, and a shift of the proton in the central hydrogen bond. This process is still fast within the NMR time scale even at low temperatures. The fact that we could not observe any ^{13}C signal in spite of the isotopic enrichment is in agreement with this interpretation: the carbon chemical shifts of the central and the terminal acetic acid residues are different;

(25) Pecul, M.; Leszczynski, J.; Sadlej, J. *J. Chem. Phys.* **2000**, *112*, 7930.

(26) Shenderovich, I. G.; Tolstoy, P. M.; Golubev, N. S.; Smirnov, S. N.; Denisov, G. S.; Limbach, H. H. *J. Am. Chem Soc.* **2003**, *125*, 11710.

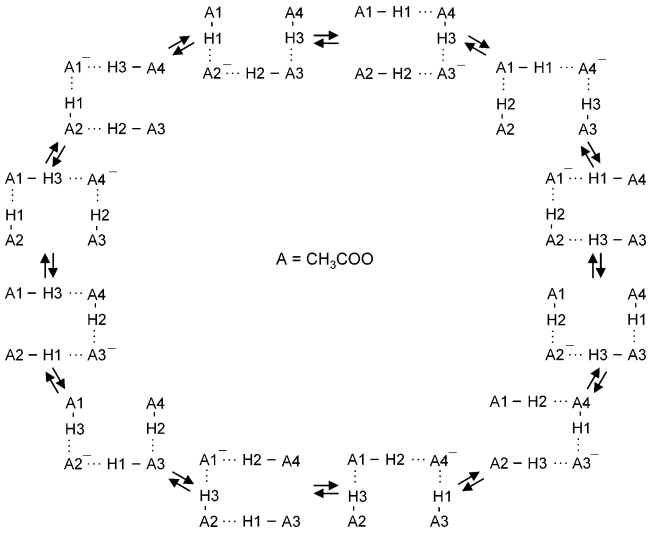

Figure 11. Proposed scheme of the 12-step exchange cycle, which makes all 3 protons in TBA trihydrogen tetraacetate magnetically equivalent in NMR time scale.

if the process is not fast enough, the ^{13}C signals will present exchange broadening, which is difficult to observe. The ^{1}H signals could be observed because the chemical shift difference between the terminal and the central protons is smaller, leading to coalesced lines at smaller exchange rate constants.

Ionization and H/D Isotope Effects on the Carboxylic Carbon NMR Chemical Shifts of Acetic Acid and Acetate in Water and Chloroform at Room Temperature. The motivation for this part of our study was to elucidate if it is possible to develop an NMR tool for deciding whether a carboxyl group of a protein is embedded in water or is located in an aprotic polar environment within the protein. This knowledge is necessary to understand the functional properties of these biomolecules. As an example, we quote the findings of Smith et al.[17] of unexpected ^{13}C chemical shifts of two specifically labeled ^{13}C catalytic carboxyl groups in the active site of HIV protease after binding of an inhibitor. The question was which conclusions concerning the protonation states of these groups can be obtained from these data. This question has been studied theoretically by Piana et al.[18]

For this purpose, we elucidated in the experiments depicted in Figures 8 and 9 the ionization shifts and the H/D isotope shifts on the acetic acid/acetate carbon chemical shifts in water and aprotic polar organic solvent. For H_2O, we observed the limiting chemical shifts of 174.8 ppm for COOH and 179.4 ppm for COO^-. This ionization ^{13}C chemical shift of +4.58 ppm observed is in good agreement with the slightly smaller values of +4.5 and +4.2 ppm observed by Hagen and Roberts[27] for concentrations of 0.5 and 2.0 M. Thus, this shift increases slightly when the solution is diluted.

For the Freon solutions at low temperatures, it was difficult to elucidate the corresponding ionization shift. Therefore, we had performed the comparative chemical shift measurements in water and chloroform depicted in Figure 9. As we started with water at pH 7 and ended up with a pH of ~9, the values observed are located within the range of the limiting chemical shifts, depending on the COO^-/COOH ratio, which increases with increasing amounts of tetrabutylammonium hydroxide. On the other hand, keeping all other conditions the same, the chemical shifts in chloroform move upfield, indicating a negative ionization shift. The signal observed corresponds to an average over various hydrogen-bonded complexes. At low tetrabutylammonium hydroxyde/acetic acid ratio, the cyclic dimer dominates, but as minor forms, some monomer and complexes with residual water also have to be discussed. At higher ratios, various complexes of the type $(AH)_nA^-$ with decreasing n are formed, which were identified in Freon solution at low temperatures. These results confirm the reversed ionization shift in organic aprotic environments, as compared to water, although no quantitative conclusions can be drawn at present.

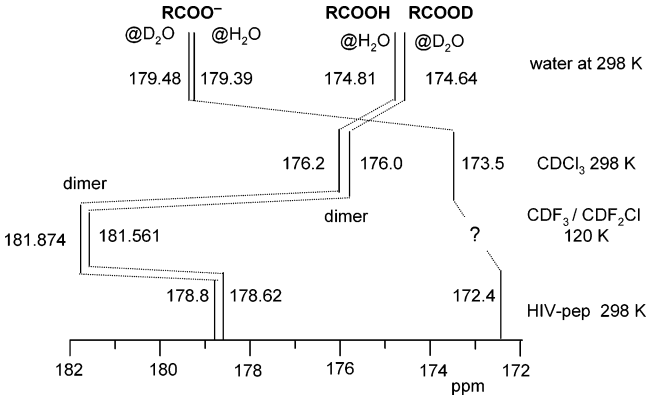

Figure 12. Evolution of ^{13}C NMR chemical shift of H and D isotopologues of acetic acid and acetate in different media. From top to bottom: water and deuterated water, chloroform, Freon mixture at low temperature, and Asp residues in HIV protease, according to ref 17.

Figure 12 gives an overview of the ^{13}C-carboxylic acid and -carboxylate chemical shifts of acetic acid in water, chloroform, and Freon solution in comparison with those of the catalytic groups of the HIV protease−inhibitor complex.[17] The reversed ionization shifts discussed above are apparent. Figure 12 also includes the chemical shift data of the carboxyl groups in the HIV−inhibitor complex. Although it is difficult to discuss the absolute chemical shift in detail, it is apparent that the "unexpected" finding of an inverse ionization shift by Smith et al.[17] indicates that the local environment of these catalytic groups corresponds to an aprotic polar rather than an aqueous environment. This interpretation supports our strategy to use liquefied Freons as model environments for the study of amino acid side-chain interactions rather than protic solvents.

Especially interesting are the H/D isotope effects on the ^{13}C chemical shifts in the different environments. For an isolated COO^- group in a polar aprotic environment, there can be no effect because of the absence of mobile hydrons. However, we observe a positive solvent isotope effect when this group is embedded at high pH in an aqueous environment. This finding is remarkable as this unexpected isotope effect occurs across the hydrogen bonds of acetate with water. On the other hand, when H is replaced by D, high-field shifts on the carboxylic acid groups are observed both for aprotic polar solvents and for an aqueous environment at low pH as indicated in Figure 12.

In a later section, we will show that the finding of no H/D isotope effect on the carboxylic/carboxylate ^{13}C chemical shift is not only compatible with the presence of an isolated carboxylate group in an aprotic environment but it can also mean that

(27) Hagen, R.; Roberts, J. D. *J. Am. Chem. Soc.* **1969**, *91*, 4504.

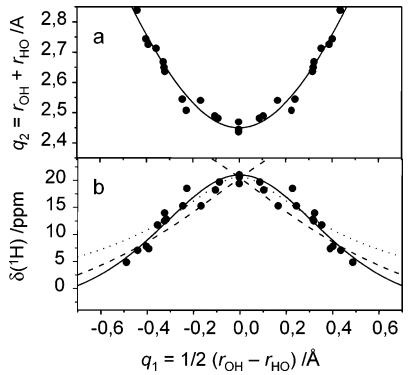

Figure 13. Hydrogen bond correlations for OHO hydrogen bonds (data points collected in ref 29). (a) q_2 vs q_1 plot; (b) ^{1}H NMR chemical shifts versus hydrogen bond asymmetry q_1 plot. Solid lines are calculated from valence bond order theory (see text) and fitted to experimental data. The dashed lines correspond to the correlations proposed in refs 29 and 32.

this group is involved in a very strong low-barrier hydrogen bond.

Hydrogen Bond Geometries and ^{1}H NMR Chemical Shifts. The question arises of how the measured ^{1}H NMR chemical shifts correlate with the hydrogen bond geometry. To establish this correlation, we will use the valence bond order model.[28] For a OHO hydrogen bond, two bond orders p_{OH} and p_{HO} can be defined, which are related via the following equation

$$p_{OH} + p_{HO} = 1 \tag{2}$$

Both bond orders decrease exponentially with the distance, i.e.

$$p_{OH} = \exp(-(r_{OH} - r^\circ)/b); \quad p_{HO} = \exp(-(r_{HO} - r^\circ)/b) \tag{3}$$

where r° represents the OH distance in the free acid molecule and b describes the decay of the bond order with increasing distance. For convenience, instead of r_{OH} and r_{HO} we will use variables q_1 and q_2, defined as

$$q_1 = (1/2)(r_{OH} - r_{HO}); \quad q_2 = (r_{OH} + r_{HO}) \tag{4}$$

For a linear hydrogen bond, q_2 corresponds to the heavy atom distance and q_1 to the displacement of the proton from the hydrogen bond center.

In Figure 13a, we have plotted the values of q_2 obtained by neutron diffraction for hydrogen bonds involving carboxyl groups, where the corresponding values of r_1 and r_2 were assembled by Sternberg and Brunner[29] as a function of the coordinate q_1. The solid line corresponds to the following equation, which has been derived previously[30] from eqs 2−4

$$q_2 = 2r^\circ - 2q_1 + 2b \ln(1 + \exp(2q_1/b)) \tag{5}$$

where the parameters are given by $b = 0.467$ Å and $r^\circ = 0.902$ Å. We note that the parameter set $b = 0.393$ Å and $r^\circ = 0.928$ Å was obtained by Steiner[31] for all kinds of OHO hydrogen bonds at temperatures below 150 K whereas $b = 0.397$ Å and $r^\circ = 0.925$ Å were obtained at room temperature.

In Figure 13b are plotted the ^{1}H chemical shift values listed in ref 29. As the fitting function for points in Figure 13b we propose the following equation, used already in a previous treatment of OHN hydrogen bonds,[30b] which correlates the proton chemical shifts with the hydrogen bond asymmetry q_1 and, therefore, also with q_2:

$$\delta(^1\mathrm{H}) = 4\Delta p_{OH} p_{HO} + \delta^\circ \tag{6}$$

In eq 6, δ° represents the ^{1}H NMR chemical shift of the "free" monomeric acid and $\Delta + \delta^\circ$ represents the maximum chemical shift of a OHO hydrogen-bonded complex. This maximum value may be reached in the case of a symmetric hydrogen bond where the proton moves in a single well potential. This is, for example, the case of hydrogen maleate containing an intramolecular symmetric OHO hydrogen bond, where the proton resonates at 20.82 ppm.[2b] As a consequence, for carboxylic acids, we set $\Delta + \delta^\circ$ to 21 ppm. Now, there is only one parameter left in eq 6, which can be obtained by a linear least-squares fitting procedure, as depicted in Figure 13b. The best fit obtained for $\delta^\circ \approx -4$ ppm and leads to the solid line in Figure 13b. However, it is unlikely that the OH proton of monomeric carboxylic acid molecules will resonate at such a high field (we remind that the experimental value for acetic acid was estimated to be +5.9 ppm[22]). Thus, δ° is a hypothetical value, describing the correlation curve of Figure 13b and connected to the model used in this work.

On the other hand, Sternberg and Brunner[29] proposed the following equation correlating proton chemical shift and hydrogen bond distance $r_{H\cdots O}$:

$$\delta(^1\mathrm{H}) = 46.5/r_{H\cdots O} - 17.5 \tag{7}$$

For comparison, we included this function in Figure 13b as broken lines. For that purpose, we had to convert the $r_{H\cdots O}$ values into q_1 values using the same valence bond order eq 3. Finally, we have included as a dotted line in Figure 13b a third correlation, proposed by Harris et al.,[32] which is based on the solid-state NMR data of McDermott and Ridenour,[33] leading to the equation

$$q_2 = 5.04 - 1.16 \ln(\delta^1\mathrm{H}) + 0.0447\delta^1\mathrm{H} \tag{8}$$

Here we assume that the value $r_{O\cdots O}$, used in ref 32, is equal to the q_2 value, which will be that of a linear hydrogen bond.

It is clear from Figure 13b that the function proposed in ref 29, having the same number of fitting parameters as the one from valence bond order theory, does not well describe the data points for the strong quasi-symmetric hydrogen bonds ($q_1 = \sim 0$). On the other hand, the function from ref 32 deviates from the experimental points for the weak hydrogen bonds ($q_1 > \sim 0.4$). We note, however, that conclusions of these authors refer to the strong hydrogen bonds, and are, therefore, valid. The advantage of the valence bond order model is that almost all parameters besides δ° are derived in an independent way.

(28) (a) Pauling, L. *J. Am. Chem. Soc.* **1947**, *69*, 542. (b) Brown, I. D. *Acta Crystallogr.* **1992**, *B48*, 553. (c) Dunitz, D. *Philos. Trans. R. Soc. London* **1975**, *B272*, 99.
(29) Sternberg, U.; Brunner, E. *J. Magn. Reson. A* **1994**, *108*, 142.
(30) (a) Benedict, H.; Limbach, H. H.; Wehlan, M.; Fehlhammer, W. P.; Golubev, N. S.; Janoschek, R. *J. Am. Chem. Soc.* **1998**, *120*, 2939. (b) Smirnov, S. N.; Benedict, H.; Golubev, N. S.; Denisov, G. S.; Kreevoy, M. M.; Schowen, R. L.; Limbach, H. H. *Can. J. Chem.* **1999**, *77*, 943.
(31) Steiner, Th. *J. Phys. Chem. A* **1998**, *102*, 7041.
(32) Harris, T. K.; Zhao, Q.; Mildvan, A. S. *J. Mol. Struct.* **2000**, *552*, 97.
(33) McDermott, A.; Ridenour, C. F. In *Encyclopedia of Nuclear Magnetic Resonance;* Grant, D. M., Harris, R. K., Eds.; John Wiley & Sons Ltd.: Chichester, U.K., 1996; p 3820.

Table 5. Geometric Parameters of the Hydrogen Bonds in the Complexes Discussed in the Paper, Obtained Using the q_1 vs δ_H Correlation. L = H, D

no.	complex	isotopologue	bond type	q_1, Å	q_2, Å	r_{OL}, Å	r_{LO}, Å
2	$(CH_3COOL)_2$	HH	OHO	−0.296	2.628	1.018	1.610
		HD	OHO	−0.299	2.633	1.016	1.615
		HD	ODO	−0.301	2.634	1.016	1.618
		DD	ODO	−0.304	2.636	1.015	1.621
3	$(CClH_2COOL)_2$	HH	OHO	−0.293	2.625	1.019	1.606
		HD	OHO	−0.295	2.627	1.018	1.609
4	$CH_3COOL\cdots{}^-OOCCH_3$	H	OHO	−0.126	2.485	1.116	1.369
		D	ODO	−0.148	2.498	1.101	1.397
5	$(CH_3COOL)_2\cdots{}^-OOCCH_3$	HH	OHO	−0.214	2.546	1.059	1.487
		HD	OHO	−0.207	2.540	1.063	1.477
6	$(CH_3COOL)_3\cdots{}^-OOCCH_3$	HHH	OHO	−0.256	2.585	1.037	1.549
		HHD	OHO	−0.253	2.583	1.038	1.545
		HDD	OHO	−0.251	2.580	1.039	1.540
7	$[C_2H_2(COO)_2L]-$	H	OHO	0	2.451	1.226	1.226
		D	ODO	0	2.451	1.226	1.226

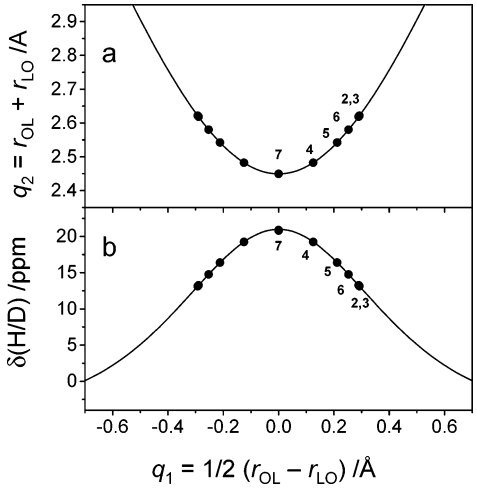

Figure 14. Hydrogen bond correlations for OHO and ODO hydrogen bonds studied in this paper. (a) q_2 as a function of q_1. (b) ^1H and ^2H NMR chemical shifts as a function of q_1. For further explanation, see test.

Finally, we note that the geometry−chemical shift correlation of eq 6 is valid for both nuclei (^1H and ^2H) at the same time only if the effects of the reduced vibrational amplitude of the deuteron and the proton on the chemical shifts are neglectable. This should be in the case of not very strong hydrogen bonds. Indeed, if the H-bond is very strong and both proton and deuteron are located close to the center of the hydrogen bond, the primary isotope effect, $\delta_D(D) - \delta_H(H)$, depends mainly on the differences between vibrational amplitudes of the proton and deuteron. It is also clear that geometries obtained for solution via a chemical shift analysis refer to those averaged over all solvent configurations. In view of all the approximations used, we do not give a margin of the experimental error, because the latter will be smaller than the systematic errors arising from the assumptions made.

Nevertheless, if we assume the validity of eqs 5 and 6, we can place the experimental chemical shifts measured in this work on the chemical shift−hydrogen bond correlation curve of Figure 13b, resulting in values of the proton coordinate q_1 as illustrated in Figure 14b. The values of q_2 and hence r_{OL} and r_{LO} are then obtained from the hydrogen bond correlation of Figure 14a. All data are assembled in Table 5. For comparison, we include the NMR parameters of hydrogen maleate TBA studied previously.[2b]

Figure 14 indicates in a nice way the shortening of the hydrogen bonds in the series from acetic acid dimer **2**, chloroacetic acid dimer **3**, trihydrogen tetraacetate **6**, dihydrogen triacetate **5**, hydrogen diacetate **4**, and hydrogen maleate **7**. All of these species exhibit either a double well or a single well potential. In the order **2**, **3**, **6**, **5**, **4**, **7**, the barrier decreases to zero. In the case of **5** and **6**, only the high-field shift of the deuteron signal as compared to the proton signal still indicates a low barrier, which is believed to be gone in the case of **7**, where the H/D isotope effect is reversed.

It would be interesting to compare the hydrogen bond geometries measured by NMR with experimental ones obtained for the gas phase. Unfortunately, we found only geometric data for acetic acid dimer **2**, which were obtained by electron diffraction.[7c] The O···O distance appeared to be 2.68 Å; this value compares well with the value found here of $q_2 = 2.628$ Å (Table 5), which would correspond to the O···O distance in the case of a hydrogen bond angle of 180°. Assuming a smaller angle would lead to a shorter O···O distance. We are tempted to assign the shorter values for the Freon solution to a shortening of the hydrogen bond induced by the solvent dipoles.

Most probably, the scattering of the data points in Figure 13b is systematic, reflecting chemical differences between various carboxylic acids; nevertheless, from this scattering, it is possible to estimate the precision of q_1 values obtained by ^1H NMR. In the region of moderately strong H-bond, we estimate the standard deviation of data points of ∼0.02 Å.

H/D Isotope Effects on the Hydrogen Bond Geometries and the Cooperativity of Hydrogen Bonds. In this section, we use the hydrogen bond correlations in order to estimate the H/D isotope effects on the hydrogen bond geometries of the hydrogen-bonded complexes studied. For this purpose, all ^1H and ^2H chemical shift data were transformed into distances. The results are included in Table 5 and depicted schematically in Charts 2−4. Chart 2 depicts the case of the homoconjugate anion **4**. We have used a cis arrangement of the non-hydrogen-bonded CO groups, because we think that this conformation will be preferred when the anion is in close contact with the tetrabutylammonium cation. However, we cannot exclude a trans conformation. The negative sign of the primary isotope effect and the single line of carboxylic carbons in the ^{13}C spectrum indicate that we have a fast conversion or proton delocalization between two asymmetric limiting structures, characterized by a short "covalent bond" and a long "hydrogen bond". On deuteration, the shorter bond becomes shorter and the longer

Chart 2. Schematic Geometry of the Hydrogen Bonds of Two Isotopologues of Hydrogen Diacetate (Acetic Acid Homoconjugate Anion 1:1)

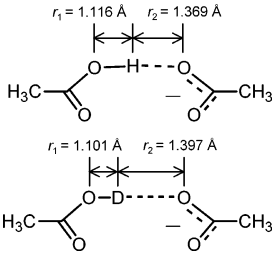

Chart 3. Schematic Geometry of the Hydrogen Bonds of Three Isotopologues of Acetic Acid Cyclic Dimer

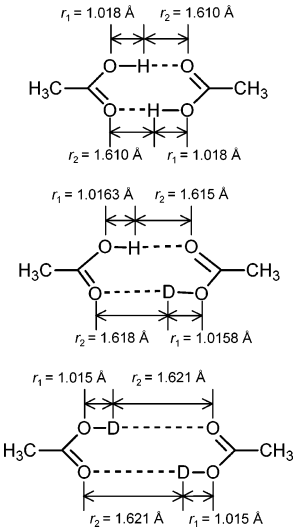

Chart 4. Schematic Geometry of the Hydrogen Bonds of Three Isotopologues of Dihydrogen Triacetate (Acetic Acid Homoconjugate Anion 2:1)

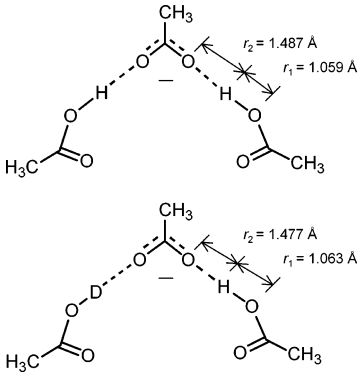

bond longer, as found previously for other hydrogen-bonded complexes.[4b,5b,26,30a]

The distance changes after partial and full deuteration of the acetic acid dimer **2** are depicted in Chart 3. Substitution of both H by D leads again to a decrease of the shorter and an increase of the longer oxygen−hydrogen distances, where the overall average symmetry of the dimer is the same in the HH and the DD isotopologues. By contrast, the symmetry of the HD species is reduced as indicated in the geometry of the HD isotopologue depicted in Chart 3. This geometry was obtained as follows.

A hydrogen-bonded proton signal of the cyclic dimer was shifted upfield when the neighboring proton was replaced by a deuteron as indicated in Figure 2; i.e., $\delta_H(HD) - \delta_H(HH) \approx -0.092$ ppm. A similar value of −0.085 ppm was observed for monochloroacetic acid dimer (Figure 3). This finding indicates a cooperativity of the two hydrogen bonds in the sense that lengthening of one hydrogen bond by H/D substitution leads also to a lengthening of the neighboring bond. Unfortunately, we were not able to determine the deuteron chemical shift of the HD isotopologue. Thus, we proceeded as follows. We noticed that the secondary isotope effects on the ^{13}C chemical shifts of both dimers were almost the same within the margin of error; i.e., $\delta_C(DD) - \delta_C(HD) \approx \delta_C(HD) - \delta_C(HH)$ (Figure 2f). Therefore, the "sum rule" for multiple isotopic substitution established in ref 4b seems to be valid for the carbon chemical shifts. We can safely assume that it is also valid for the hydron chemical shifts, i.e., that $\delta_H(HH) + \delta_D(DD) = \delta_H(HD) + \delta_D(HD)$. As the values of $\delta_H(HH) = 13.13$ ppm, $\delta_H(HD) = 13.04$ ppm, and $\delta_D(DD) = 12.83$ ppm for Freon solutions around 110 K were known, we could then obtain the value of $\delta_D(HD) = 12.92$ ppm, leading to the distances of the HD isotopologue in Chart 3.

In contrast to acetic acid cyclic dimer **2**, the hydrogen bonds in dihydrogen triacetate **5** are anticooperative. This is manifested in a low-field shift of a given hydrogen bond proton signal upon deuteration of the neighboring bonds (Figure 5). The corresponding geometric change of this OHO group is indicated in Chart 4. Now, the shorter OH distance is lengthened and the longer H···O distance shortened. Unfortunately, we were not able to establish the geometric changes of the ODO group in a quantitative way, as the deuterium signal of the HD species could not be resolved (Figure 5).

A smaller low-field vicinal isotope effect was observed in the case of the trihydrogen tetraacetate **6** (Figure 7). However, this effect could not be quantitatively analyzed because it represents an average of the central and the terminal hydrogen bonds in this species, due to the fast fluxional process depicted in Figure 11.

H/D Isotope Effects on the ^{13}C Chemical Shifts. Having established the hydrogen bond geometries of the various species, we can now ask the question of how the ^{13}C NMR parameters are related to the hydrogen bond geometries. For the chemical shifts, we could not establish a clear dependence. However, a correlation was obtained for the H/D isotope effects on the carboxylic acid carbons as shown as follows.

In a first step, we have plotted in Figure 15a these effects, Δ_{exp}, listed in the second column of Table 6 as a function of the ^1H chemical shifts of the hydrogen bond protons. We include the value of the adduct **1** of acetic acid with $SbCl_5$ as limiting value for the case of the absence of a hydrogen bond. Here, a weak upfield shift of ∼−0.1 ppm is observed. When a hydrogen bond is formed, the isotope effect decreases to −0.31 ppm after complete deuteration in the doubly deuterated cyclic dimer **2**, which is a typical value for the carboxylic acid dimers.[34] The effect increases then to −0.25 ppm for **5**, to −0.2 ppm for **4**, and toward zero for **7**, the strongest no-barrier hydrogen-bonded system. The dashed line is a guide for the eye, which represents qualitatively the evolution of the isotope effect. Unfortunately, we were not able to obtain isotope shifts for defined hydrogen-bonded complexes where the proton has crossed the hydrogen bond center, i.e., is far away from the carboxylate group. We

(34) Ladner, H. K.; Led, J. J.; Grant, D. M. *J. Magn. Reson.* **1975**, *20*, 530.

Table 6. Experimental and Corrected Isotope Effects on ^{13}C NMR Chemical Shifts of the Complexes Discussed in the Paper. L = H, D

compound	Δ_{exp}, ppm	degenerate process	equation	q_1, Å	Δ_{COO-}, ppm	Δ_{COOL}, ppm
$CH_3COOL{\cdot}SbCl_5$	−0.096[a]			−inf.		−0.096
$(CH_3COOL)_2$	−0.313[b]	HH transfer	process does not modulate Δ	−0.296		−0.313
$(CClH_2COOL)_2$	−0.276[b]	HH transfer	process does not modulate Δ	−0.293		−0.276
$(CH_3COOL)_2{\cdots}^-OOCCH_3$	−0.25[b]	H-bond exchange	$\Delta = 2\Delta_{COOL}/3+\Delta_{COO-}/3$	−0.214	$0<\Delta_{COO-}<+0.07$	$-0.375>\Delta_{COOL}>-0.41$
$CH_3COOL{\cdots}^-OOCCH_3$	−0.20[a]	H transfer	$\Delta=\Delta_{COOL}/2+\Delta_{COO-}/2$	−0.126	$0<\Delta_{COO-}<+0.07$	$-0.4>\Delta_{COOL}>-0.47$
$[C_2H_2(COO)_2L]^-$	−0.07[a]	single well	$\Delta=\Delta_{COOL}/2+\Delta_{COO-}/2$ $\Delta_{COOL}=\Delta_{COO-}$	0	−0.07	−0.07

[a] $\Delta = \delta_C(D) - \delta_C(H)$, [b] $\Delta = \delta_C(DD) - \delta_C(HH)$. Δ_{exp}, experimental value; Δ_{COO-} and Δ_{COOL}, intrinsic values

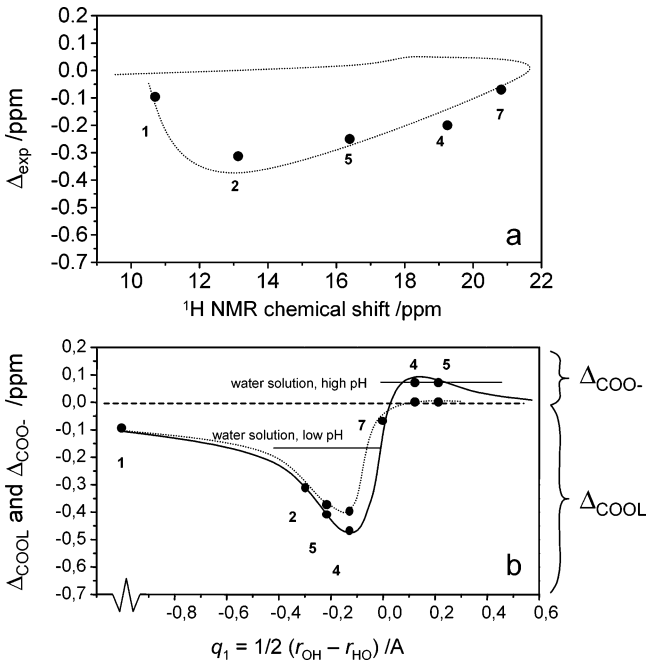

Figure 15. H/D isotope effect on carboxylic ^{13}C NMR chemical shift as a function of (a) ^1H NMR chemical shift and (b) hydrogen bond asymmetry q_1 (experimental values of isotope effects corrected for the exchange processes. See text for more details) for acetic acid complexes and TBA hydrogen maleate.

can, however, estimate the behavior of the correlation line for COO^- anion. After the quasi-symmetric hydrogen bond is formed, further proton transfer to the base will result in the hydrogen bond weakening; i.e., ^1H signals will shift upfield and in the limit of no hydrogen bond, for isolated carboxylate, the line will go to zero. For intermediate values, the isotope effect may become slightly positive, as indicated by the positive effect of carboxylate in water. Unfortunately, we could not place this point in the diagram of Figure 15a as we do not know the ^1H chemical shift of the water molecules solvating this anion. This correlation may be of help in the future to estimate the ^1H chemical shifts of a hydrogen-bonded carboxylic acid side-chain from the H/D isotope effects on the $COOH/COO^-$ chemical shift.

The correlation with the hydrogen bond coordinate q_1 depicted in Figure 15b was obtained in a second step as follows. The problem was that we had to take the fluxional processes in the different complex into account in order to obtain the intrinsic values of the isotope effects on the ^{13}C chemical shifts. An overview is given in Table 6. The degenerate processes occurring in **2** and **3** are the double proton transfers, in **4** a single proton transfer, and in **5** and **6** the H-bond exchange processes depicted in Figures 10 and 11. The corresponding expressions for the average H/D isotope effects are included in the columns 5 and 6, where Δ_{COOL} represents the intrinsic effect in the region where the H-bonded proton is closer to the carbon studied, and Δ_{COO-} the effect across the hydrogen bond for the particular species.

To calculate Δ_{COOL} we need the values of Δ_{COO-}. We estimate the latter in the range between 0 and +0.07 ppm found for acetate in water. Using this range, we can calculate the range of the intrinsic values of Δ_{COOL} listed in the last column of Table 6. These values are plotted in Figure 15b as a function of the values of the hydrogen bond coordinate q_1 obtained in Figure 14. The dashed and the solid lines are again guides for the eye and represent the range of the possible values of H/D substitution on the ^{13}C chemical shifts of COOH and COO^-.

The new correlation indicates a deep minimum when the proton is moved toward the hydrogen bond center and a rapid decrease to zero when the proton crosses the center. After crossing the center, the effect is zero in the entire range of positive q_1 values and exhibits intermediately slightly positive values as found for water, leading to a distorted dispersion-like curve. We note that symmetric dispersion curves were observed previously for nitrogen nuclei involved in NHN[30a] or NHO hydrogen bonds.[35]

Using this correlation, we can estimate the hydrogen bond geometries of the COOH and COO^- in water. For COOH, two values of q_1 are consistent with the correlation, i.e., around −0.5 and −0.05 Å, whereas for COO^-, we estimate values between +0.1 and +0.2 Å. However, we note that the values for water do not refer to a single hydrogen bond but to multiple bonds, and one could argue that these values cannot be included in the correlation of Figure 15b.

The use of the correlation can be demonstrated in the case of the HIV−pepstatin complex mentioned in a previous section. The values of -0.18 ± 0.04 ppm and of ~0 ppm observed by Smith et al.[17] for the two ^{13}C-labeled aspartic acid residues indicate the following. The structure of the first COOH group is compatible with a value of $q_1 \approx -0.5$ Å or with a value of $q_1 \approx 0$ Å. If the latter is true, the structure of the second group must be also involved in a strong hydrogen bond, but the proton has slightly shifted across the hydrogen bond center to positive, so far unknown values of q_1. This even incomplete information supports the suggestion of Northrop[16c] of a low-barrier hydrogen bond between the two carboxylic groups of HIV protease and

(35) Lorente, P.; Shenderovich, I. G.; Buntkowsky, G.; Golubev, N. S.; Denisov, G. S.; Limbach, H. H. *Magn. Reson. Chem.* **2001,** *39,* S18.

might be of great help in the future for theoretical studies of this and related systems.[18]

Conclusions

The main conclusion of this study of hydrogen-bonded species of acetic acid dimers and complexes with acetate is that a combination of low-temperature ^{1}H, ^{2}H, and ^{13}C NMR spectroscopy of the nondeuterated, partially, and fully deuterated complexes allows one to obtain various NMR parameters that provide information about the hydrogen bond structures, geometries, and fluxional processes in solution. Complementary studies of acetic acid in water indicate an inverse ionization shift of the carboxyl group in water and in polar solvent, which has been also observed for the active site of the HIV−pepstatin complex.[17] This means that acid−base interactions between amino acid side chains of proteins are better modeled using aprotic polar solvents such as the Freon mixture CDF_3/CDF_2Cl employed in this study rather than an aqueous or protic environment. A correlation of the H/D isotope effects on the chemical shifts of carboxyl/carboxylate groups with the hydrogen bond geometries and protonation states has been derived from the model complexes studied here, which provides a novel way to obtain information about the local environment and the protonation state of a carboxyl group, i.e., aqueous environment with two protonation states, COOH and COO^-, or an aprotic polar environment with a multitude of hydrogen bond geometries.

Acknowledgment. This research has been supported by the Deutsche Forschungsgemeinschaft, Bonn, the Fonds der Chemischen Industrie (Frankfurt), and the Russian Foundation of Basic Research, Grants 03-03-04009 and 03-03-32272. P.M.T. is indebted to the Fonds der Chemischen Industrie for a Kékulé Fellowship.

JA039280J